# Experimental determination of the optimum intermediate and gas-cooler pressures of a commercial transcritical $CO_2$ refrigeration plant with parallel compression.

**Laura Nebot-Andrés*, Daniel Sánchez, Daniel Calleja-Anta, Ramón Cabello, Rodrigo Llopis**

Thermal Engineering Group, Mechanical Engineering and Construction Department,
Jaume I University, Spain

*Corresponding author: lnebot@uji.es, +34 964 718133

## Abstract

$CO_2$ systems used in refrigeration are becoming more complex with the aim of improving their energy performance. Parallel compression is one of the implemented solutions to enhance the performance of the plants. However, an optimization process is required to operate this system at high performance and its operation is subjected to physical limitations in real plants.

This work presents the experimental optimization of a transcritical $CO_2$ plant working with parallel compression. The plant is tested at different discharge pressures and different secondary compressor speeds in order to optimize the COP of the plant and determine the optimal conditions for three gas-cooler exit temperatures 27.5ºC, 32.5ºC and 37.5ºC and three evaporation levels: -15.0ºC, -10.0ºC and -5.0ºC.

The optimal working conditions that can be achieved in a real plant have been determined, obtaining COP from 1.71 to 2.63 for -5.0ºC, from 1.50 to 2.22 for -10.0ºC and from 1.25 to 1.84 for -15.0ºC. Cooling capacity ranges from 8.94 kW to 11.34 for -5.0ºC, from 7.71 kW to 9.47 kW for -10.0ºC and from 6.22 kW to 7.76 kW for -15.0ºC. The trends observed in theoretical results have been corroborated and the optimum gas-cooler and intermediate pressures have been determined and discussed.

## Keywords

Carbon dioxide, COP, energy improvement, parallel compression, optimization

## Nomenclature

| | |
|---|---|
| BP | back-pressure valve |
| COP | coefficient of performance |
| h | specific enthalpy, $kJ \cdot kg^{-1}$ |
| $\dot{m}$ | mass flow rate $kg \cdot s^{-1}$ |
| MT | medium temperature |
| p | absolute pressure, bar |
| Pc | power consumption, kW |
| PID | proportional–integral–derivative controller |
| Q | cooling capacity, kW |
| t | temperature, ºC |

**Greek symbols**

| | |
|---|---|
| $\varepsilon$ | uncertainty |
| $x$ | vapour quality |

**Subscripts**

| | |
|---|---|
| dep | corresponding to the liquid tank |

| | |
|---|---|
| dis | compressor discharge |
| gc | gas-cooler |
| i | intermediate |
| in | inlet |
| main | corresponding to the main cycle |
| 0 | evaporating level |
| o | outlet |
| PC | corresponding to the parallel compressor |
| w | water |

## 1. Introduction

Centralized Commercial refrigeration has undergone several technological advances in recent years that have been driven by different regulations that restrict the use of certain refrigerants in these facilities. First advances were driven by the Montreal Protocol, the Kyoto Protocol and the subsequent Kigali Amendment [1]. After the F-Gas regulation [2], $CO_2$ is the only gas that meets the limitations and can be used in these plants in safety conditions since it is neither toxic nor flammable. Although it is a perfect fluid to meet legislative restrictions, its performance in basic systems is not as good as that of other fluorinated gases.

Researcher's efforts have been focused on improving the performance of $CO_2$ systems in order to make them more competitive. Several research lines have been studied, as the use of ejectors [3-5], the subcooling methods [6] as the internal heat exchanger [7], the dedicated mechanical subcooling [8-11] and the integrated mechanical subcooling [12], the combination with other systems [13-15] and the parallel compression [16]. This latter is one of the most implemented solutions in commercial refrigeration.

Sawalha et al. [17] investigated the refrigeration performance of three $CO_2$ transcritical solutions based on field measurements and saw that transcritical booster systems with gas removal from the intermediate vessel have the highest total COP at that moment. Later, authors studied the integration of heating and air conditioning into a $CO_2$ transcritical booster system with parallel compression in a Swedish supermarket and obtained an increment of 8% on the total COP comparing with the system without PC [13, 18].

Gullo el al. [19], compared several supermarket configurations, including the parallel compression, located in cities with warm climates. They found that all the enhanced configurations obtained a comparable energy saving to the one of the cascade system for the studied locations.

Tsamos et al. [20] compared four different $CO_2$ refrigeration system configurations for the weather conditions of London, UK, and Athens, Greece. They found the $CO_2$ booster with parallel compressor to be the most energy efficient system for moderate and warm climates. Energy efficiency improvement over the conventional $CO_2$ booster was of 5.0% for the warm climate and 3.6% for the moderate climate.

The parallel compression is widely applied in booster systems for supermarket applications and combined with other systems as heat recovery [21]. The parallel compression is also combined with ejectors in European food retail industry [22].

However, there are not many studies that analyze the behavior of the parallel compression and its improvement applied to a simple cycle. In supermarket boosters with PC only the heat rejection pressure is controlled, since the pressure of the receiver is maintained around 35 bars [23].

Sarkar and Agrawal [16] performed a theoretical optimization study of a transcritical $CO_2$ refrigeration cycle with parallel compression economization, comparing three different techniques: parallel compression

economization alone, parallel compression economization with recooler and multistage compression with flash gas bypass. They obtained an increment of 47.3% in terms of COP thanks to the parallel compression economization.

Minetto et al. [24] performed a theoretical investigation of a transcritical refrigerating $CO_2$ cycle with parallel compression and found benefits on the COP and cooling capacity when compared with the traditional cycle. Moreover, the optimum intermediate pressure is lower and the gas-cooler pressure is also lower than the optimal one for the traditional cycle.

Later, Chesi et al. [25] performed an experimental analysis of a $CO_2$ parallel compression cycle in flash tank configuration. In the first part, the authors carried out a theoretical study to define the limitations of the system and later performed the experimental tests but without optimizing the intermediate pressure. The tests were performed with a fixed parallel compressor speed, so the intermediate pressure is not optimized and the maximum improvements have not been reached.

Bella and Kaemmer [26] presented the experimental evaluation of a reciprocating prototype working with $CO_2$ with parallel compression. The compressor is a semi-hermetic four cylinders compressor with one compression chamber. Authors highlighted the influence of the intermediate pressure on the efficiency of the compressor and the system. They also found that the compressor shows a degradation in performance when the intermediate pressure increases.

Literature shows that there are no experimental studies in which the two working pressures are optimized at the same time, since in booster systems the tank pressure remains constant and Chesi et al. [25] also limit this variable.

The objective of this work is to determine experimentally the optimum conditions of $CO_2$ refrigeration plant with parallel compression, working in transcritical conditions. The main objective is to identify the existence of these optimal conditions and determine which are the needed pressures, gas-cooler pressure and intermediate pressure, to obtain the maximum COP of the installation. The results presented on this paper correspond to the evaluation of the plant at three different evaporation levels (-15.0ºC, -10.0ºC and -5.0ºC) and three gas-cooler exit temperatures (27.5ºC, 32.5ºC and 37.5ºC), determining for each test the optimum values of gas-cooler and intermediate pressures. The applicability of this study focuses on medium temperature (MT) applications or in the high temperature cycle of a booster cycle.

Optimum conditions have been determined and stated on a general expression depending on the evaporation temperature and the temperature at the exit of the gas-cooler. The evolution of the main energy parameters is analyzed as well as the behavior of the optimum working conditions.

## 2. Refrigeration cycle and description of the experimental plant

The transcritical refrigeration plant with parallel compressor is presented in this section. The scheme of the plant and the Ph diagram of the cycle are shown in Figure 1. The refrigeration system is made up of two compressors: a main compressor and a secondary compressor (PC) that extracts vapour from the tank and recompresses it at the gas-cooler inlet. From the vessel, saturated liquid is extracted and expanded until the evaporator. The aim of the secondary compressor is to reduce the intermediate pressure ($p_i$) in order to increase the specific cooling capacity of the evaporator.

Although the use of the PC has benefits in the behaviour of the cycle, it must also be taken into account that the presence of an additional compressor represents an increase in power consumption. Therefore, a compromise must be found between the power consumption and the intermediate pressure, for which the use of the PC enhances the COP.

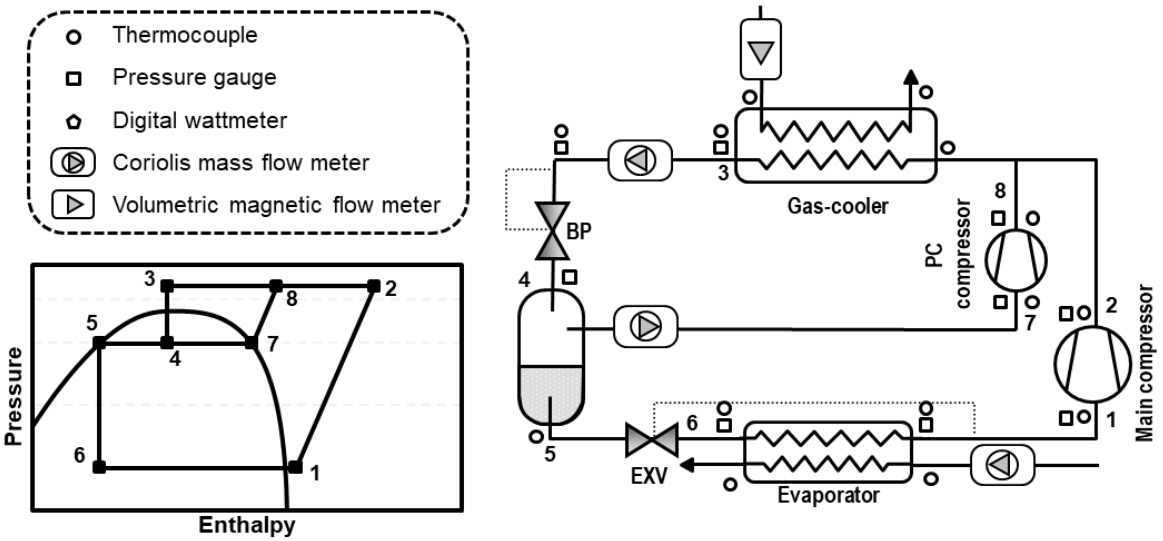


Figure 1. Schematic of the experimental plant and the measurement system and Ph diagram of the cycle.

### 2.1. Experimental plant

The schematic figure of the plant tested in this work is shown in Figure 1, and the experimental plant in Figure 2. The plant is a $CO_2$ single-stage transcritical refrigeration system with a parallel compressor system, extracting gas from the vessel. The main single-stage refrigeration cycle uses a semihermetic compressor with a displacement of 3.48 $m^3 \cdot h^{-1}$at 1450 rpm and a nominal power of 4 kW. The expansion is carried out by a double-stage system, composed of an electronic expansion valve (back-pressure) controlling the gas-cooler pressure, a liquid receiver between stages and an electronic expansion valve that controls the degree of superheat in the evaporator. Evaporator and gas-cooler are brazed plate counter current heat exchangers with exchange surface area of 4.794 $m^2$ and 1.224 $m^2$, respectively. The parallel compressor is a variable speed semihermetic compressor with displacement of 1.12 $m^3 \cdot h^{-1}$ at 1450 rpm.

Heat dissipation in gas-cooler is done with a water loop, simulating the heat rejection level. The evaporator is supplied with another loop, working with a propylene glycol–water mixture (60% by volume). Both the mass flow and the inlet temperature of the two secondary fluids can be controlled in these loops.

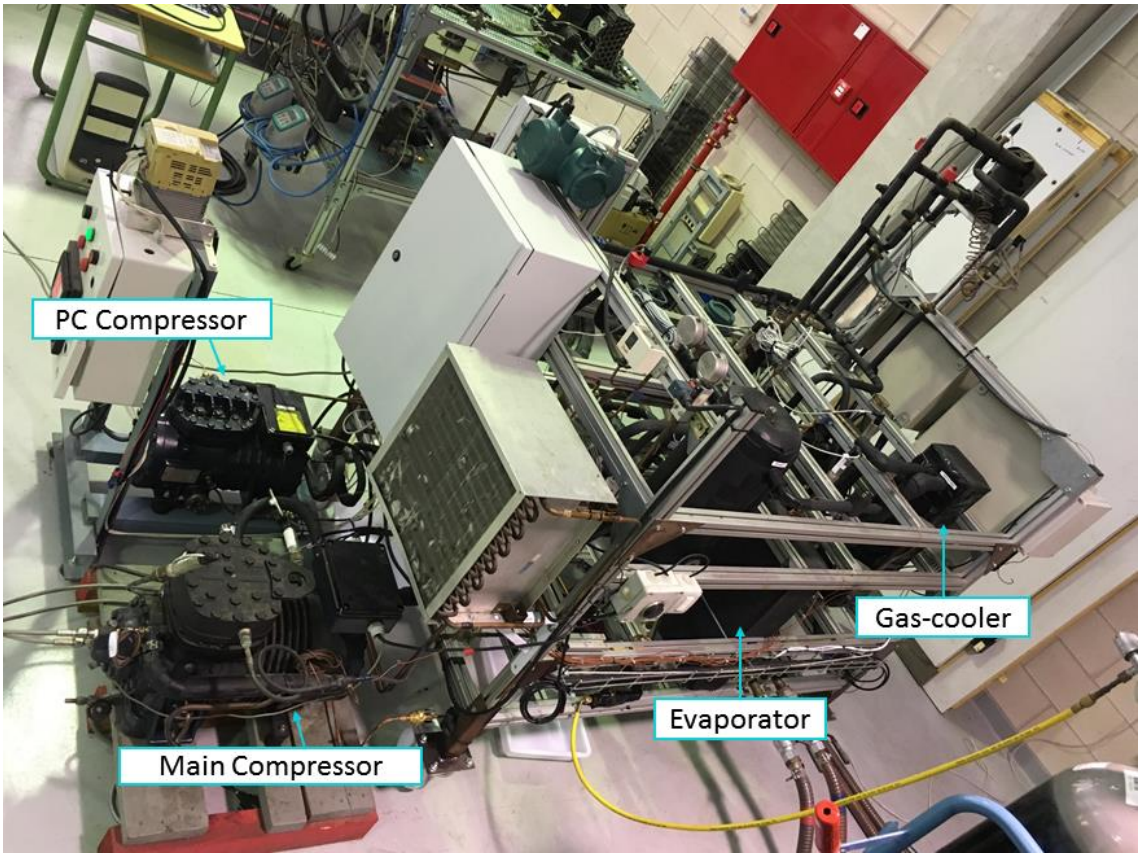


Figure 2. Experimental $CO_2$ plant.

### 2.2. Measurement system

The thermodynamic properties of the working fluids are obtained thanks to the measurement system presented in Figure 1. All fluid temperatures are measured by 18 T-type thermocouples. The majority of the thermocouples are surface thermocouples but the ones placed at the evaporator, the exit of gas-cooler and subcooler are immersion thermocouples. Pressures are measured with 11 pressure gauges installed along all the circuit. $CO_2$ mass flow rates are measured by two Coriolis mass flow meters, as well as dissipation flow on the evaporator, which is measured by another Coriolis mass flow meter. The water flow of the gas-cooler dissipation is measured using a magnetic volumetric flow meter. Power consumptions of the compressors are measured by two digital watt meters. The accuracies of the measurement devices are presented in Table 1.

Table 1. Accuracies and calibration range of the measurement devices.

| Measured variable | Measurement device | Range | Calibrated accuracy |
|---|---|---|---|
| Temperature (ºC) | T-type thermocouple | -40.0 to 145.0 | ±0.5K |
| $CO_2$ pressure (bar) | Pressure gauge | 0.0 to 160.0 | ±0.6% of span |
| $CO_2$ pressure (bar) | Pressure gauge | 0.0 to 100.0 | ±0.6% of span |
| $CO_2$ pressure (bar) | Pressure gauge | 0.0 to 60.0 | ±0.6% of span |
| $CO_2$ main mass flow rate ($kg \cdot s^{-1}$) | Coriolis mass flow meter | 0.00 to 1.38 | ±0.1% of reading |
| $CO_2$ PC mass flow rate ($kg \cdot s^{-1}$) | Coriolis mass flow meter | 0.00 to 0.083 | ±0.1% of reading |
| Water mass flow rate ($m^3 \cdot h^{-1}$) | Magnetic flow meter | 0.0 to 4.0 | ±0.25% of reading |
| Glycol volume flow rate ($kg \cdot s^{-1}$) | Coriolis mass flow meter | 0.00 to 13.88 | ±0.1% of reading |
| Power consumption (kW) | Digital watt meter | 0.0 to 6.0 | ±0.5% of reading |

## 3. Experimental tests

The strategy for conducting the experimental tests in order to determine the optimum conditions is presented in this section.

### 3.1. Test procedure

To evaluate the refrigeration $CO_2$ plant working with parallel compressor, the system has been tested at different evaporation levels and different gas-cooler outlet temperatures. The evaluated conditions are:

- Three different evaporation temperatures: -5.0, -10.0 and -15.0ºC with maximum measured deviation of ±0.20°C. The evaporation level is maintained adjusting the inlet temperature of the secondary fluid and the flow rate. The secondary fluid is a mixture propylene glycol-water (60% by volume).

- Three different gas-cooler exit temperatures: 27.5, 32.5 and 37.5°C, with maximum measured deviation of ±0.20°C. The heat rejection was performed with the secondary fluid (water) that can be controlled in terms of flow rate and inlet temperature.

- Gas-cooler pressure was regulated with an electronic Back-Pressure (BP). The pressure is fixed during each test and it is controlled thanks to a PID controller. Each test was performed at different pressures in order to identify the optimum one and reach the optimum COP conditions.

- Compressors: The main compressor always operated at nominal speed of 1450 rpm. The speed of the PC compressor was varied to modify the intermediate pressure.

- Electronic expansion valve: The electronic expansion valve of the evaporator was set to obtain a superheating degree in the evaporator of 10K.

Tests were carried out in steady state conditions for periods longer than 10 minutes, taking data each 5 seconds, obtaining the test point as the average value of the whole test. The measured data was used to calculate the thermodynamic properties of the cycle points using Refprop v.9.1. [27].

### 3.2. Test range

Table 2 sums up the range of evaluated conditions for all the test including intermediate and gas-cooler pressures, COP and cooling capacity. The number of tests carried out for each evaluated condition is also included on the table, with a total number of tests of 152.

Table 2. Experimental tests and range of tested conditions.

| $t_{gc,o}$ (ºC) | $t_o$ (ºC) | number of tests | $P_i$ (bar) | $P_{gc}$ (bar) | COP (-) | $Q_0$ (kW) |
|---|---|---|---|---|---|---|
| 27.5 | -5.0 | 19 | 44.3-49.0 | 75.4-76.1 | 2.57-2.63 | 11.0-11.5 |
| | -10.0 | 14 | 35.0-46.5 | 75.0-79.9 | 1.99-2.22 | 9.0-9.8 |
| | -15.0 | 13 | 33.2-43.6 | 74.4-80.9 | 1.67-1.84 | 7.4-8.2 |
| 32.5 | -5.0 | 12 | 44.3-64.4 | 79.7-94.9 | 1.87-2.24 | 8.5-10.6 |
| | -10.0 | 24 | 43.1-60.5 | 78.5-84.9 | 1.58-1.84 | 7.4-8.9 |
| | -15.0 | 12 | 42.1-54.0 | 77.4-80.9 | 1.49-1.58 | 6.4-7.2 |
| 37.5 | -5.0 | 21 | 49.1-67.2 | 90.1-97.0 | 1.62-1.71 | 7.7-9.7 |
| | -10.0 | 19 | 46.7-67.4 | 86.8-91.9 | 1.34-1.50 | 6.1-8.1 |
| | -15.0 | 18 | 44.8-58.4 | 85.9-90.8 | 1.12-1.26 | 5.7-6.5 |

## 4. Optimization of the plant

The cooling capacity of the cycle is calculated as the product of the $CO_2$ mass flow rate and the enthalpy difference between the exit and the entrance of the evaporator, as stated in Eq. ( 1 ). The enthalpy at the entrance of the evaporator is considered to be the same as the enthalpy at the exit of the vessel, before the expansion valve, as shown in Eq. ( 2 ). This enthalpy is calculated with the value of the pressure in the liquid tank and considering saturated liquid. To guarantee consistency of calculations, it was verified in each test that the refrigerant at the exit of the vessel was saturated liquid, as it can be seen in Figure 3.

$$\dot{Q}_0 = \dot{m}_0 \cdot (h_{0,o} - h_{0,in}) \quad (1)$$

$$h_{0,in} = h_{dep,liq} = f(P_i, x = 0) \quad (2)$$

$$h_{0,o} = f(P_{0,o}, t_{0,o}) \quad (3)$$

Figure 3. $CO_2$ liquid level in the vessel.

The COP of the plant is evaluated as the ratio between the cooling capacity and the power consumption of both compressors:

$$COP = \frac{\dot{Q}_0}{Pc_{main} + Pc_{PC}} \quad (4)$$

### 4.1. Determination of the optimum COP

$CO_2$ transcritical cycles can be performed at maximum efficiency by optimizing the gas-cooler pressure but, when having a parallel compressor, it is also necessary to optimize the intermediate pressure [28]. In $CO_2$

cycles with parallel compression, lower intermediate pressures increase the specific cooling capacity of the system but also the compression ratio and mass flow of the PC compressor are higher.

The tests have been performed in order to identify the maximum COP. First, three points are tested for different gas-cooler and intermediate pressures, always values close to those obtained in previous theoretical studies. Then, the three first tested points are represented in a graph and from there; a colour map is formed by these three points, similar to that presented in Figure 4. The intermediate pressure or gas-cooler pressure values are modified in the direction where the COP increases as it is indicated in the contour map. This procedure is followed, obtaining new COP points until the maximum COP is clearly identified. Both gas-cooler pressure and intermediate pressure can be modified independently according to the needs of each tested condition. New points are added to the colour map and the process ends when the increments achieved between the new COP value and the previous one are less than 1%.

Figure 4 shows the COP for the evaporating temperature of -5.0ºC and a gas-cooler outlet temperature of 27.5ºC. COP is presented as a function of the gas-cooler and the intermediate pressures. The optimum point has been marked with a blue circle. It corresponds to an intermediate pressure of 46.0 bar and 75.4 bar in gas-cooler. It can be seen that as the intermediate pressure increases or decreases with respect to the optimum, the COP decreases. Similar trend is observed regarding the gas-cooler pressure, when gas-cooler pressure increases, the COP decreases. Gas-cooler pressures under 74.4 bar have not been tested because the aim of this work is only to evaluate the system in transcritical conditions.

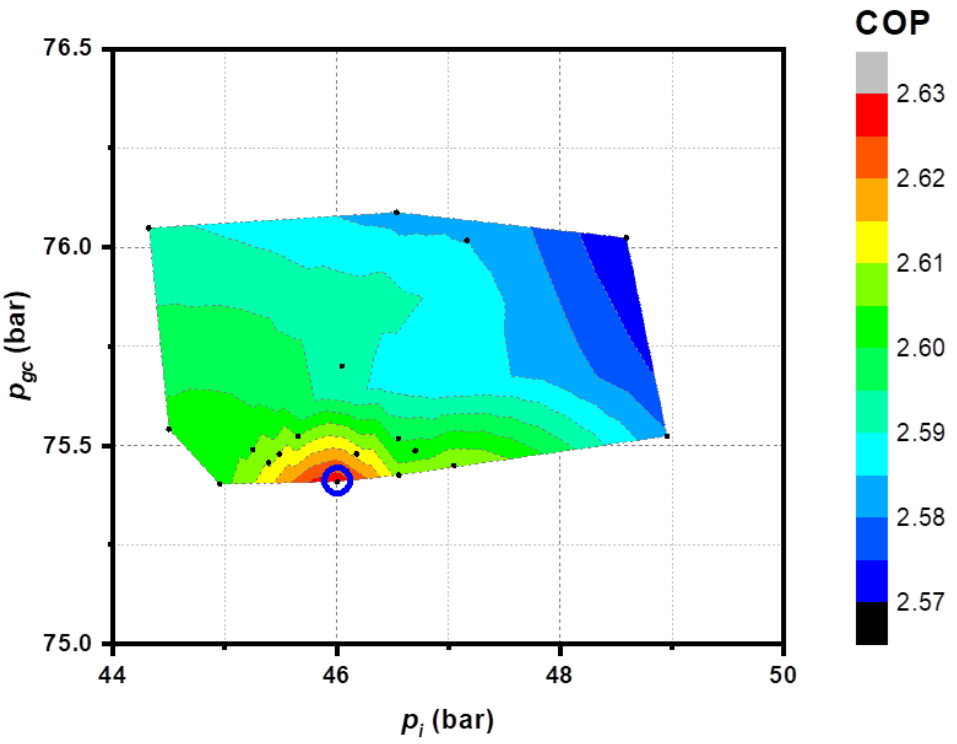


Figure 4. COP as a function of gas-cooler and intermediate pressure for $t_0$ =-5.0ºC $t_{gc,o}$=27.5ºC.

As it can be seen in Figure 4 and later in Figure 6, the effect of the gas-cooler pressure in the COP is higher than the effect of the intermediate pressure. Modifying the pressure with respect to its optimal value, we can see that the COP decreases. As illustrative data, observing Figure 4 and Figure 6 we can see that a variation of 5 bars in the intermediate pressure has less effect on the COP than a variation of 5 bar in the gas-cooler pressure, where the COP would suffer a more important reduction.

Cooling capacity is inversely related to the intermediate pressure. When higher the intermediate pressure is, lower the cooling capacity is. Conversely, cooling capacity is not much dependent on the gas-cooler pressure. As it can be seen in Figure 5, for a fixed intermediate pressure, cooling capacity remains the same regardless of the gas-pressure. However, this phenomenon only occurs when analysing very small gas-cooler variations. This is because the influence of the intermediate pressure on the cooling capacity is much higher than the influence of gas-cooler pressure. Analysing a higher range of gas-cooler pressures has an effect on the cooling capacity of the plant.

The evolution of the cooling capacity as a function of both pressures can be seen in the Figure 5. The colour map shows the evolution of the cooling capacity for $t_0$ =-5.0ºC and $t_{gc,o}$=27.5ºC. The point corresponding to the maximum COP obtained in Figure 4 is marked in blue.

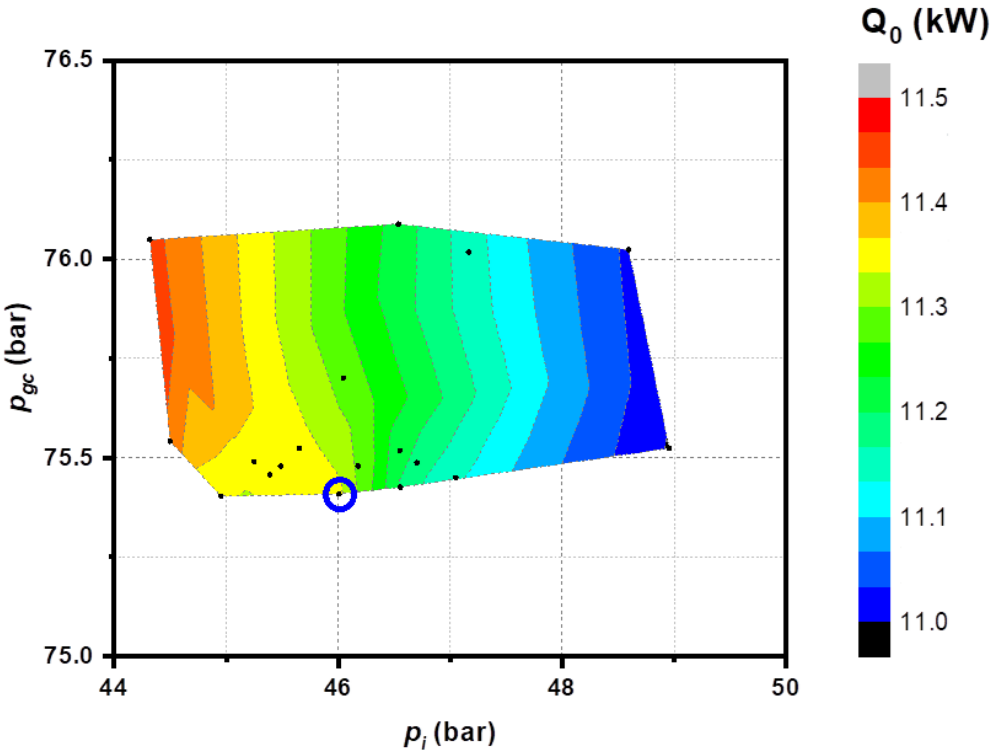


Figure 5. Cooling capacity for $t_0$ =-5.0ºC $t_{gc,o}$=27.5ºC

From this moment on, all the data presented are obtained following the process above described and correspond to the optimum point of each of the studied test conditions.

### 4.2. Physical limitations of the plant

During the experimental evaluation of the plant, some physical limits have been detected. As previously mentioned, gas-cooler pressure is regulated thanks to the backpressure valve. For each gas-cooler outlet and evaporator temperatures, there is a lower gas-pressure limit from which it is impossible to make pressure go lower. As it can be seen in Figure 6, this low limit is different depending on the gas-cooler outlet temperature. It can be seen that the optimum point is located at this low limit. When higher the gas-cooler outlet temperature is, higher the limit pressure is. The evaporator level has little influence on this parameter as it will be presented later in Figure 10, where the optimum gas-cooler pressures are represented.

The reason for that phenomenon is the mass balance in the liquid tank. As mentioned in the previous section, saturated liquid must be extracted from the lower part of the tank and saturated vapor from the upper part to ensure the correct operation of the system. Also, the system should be evaluated in steady-state conditions; otherwise, the mass balance in the tank (Eq. ( 5 )) is not verified.

Hazarika [29] studied the receiver influence in $CO_2$ air-conditioning two-stage expansion unit. Authors found that higher the size of the receiver is, higher will be the range of refrigerant charge over which the liquid portion changes from 0 to 100% in the receiver. Thus, for a specific size of receiver, the refrigerant charge should be maintained within the range to keep the receiver partially filled with liquid during operation. This means that if the refrigerant charge is lower than the lower limit of that range, we cannot ensure the presence of liquid in the tank. And if the refrigerant charge is higher than the upper limit of that range, we would have 100% liquid in the tank. Working within the limits of this refrigerant charge range ensures that the tank pressure will remain constant regardless of the refrigerant charge. For the experimental tests presented in this work, the refrigerant charge has been maintained and also corroborated that it is inside the correct range for the real liquid receiver.

Chesi et al. [25] demonstrated that for a given condition ($t_{g,co}$, $p_{gc}$ and $t_0$) and given conditions of the compressors, there is only one possible intermediate pressure that ensures both conditions stated in the previous paragraph, because after expanding from the gas-cooler exit and entering to the vessel, the $CO_2$ quality changes when the intermediate pressure is varied. As presented by some authors [24, 25], the intermediate pressure of this cycle is influenced by the compressor volumetric flow ratio. It means that the intermediate pressure is affected by the range of compressors volumetric ratio that the plant can realize. This determines the operability limits of parallel compression cycle by the choice of the compressors.

That is why the physical limits of the system depend on the gas-cooler conditions but also on the sizes and performances of the compressors.

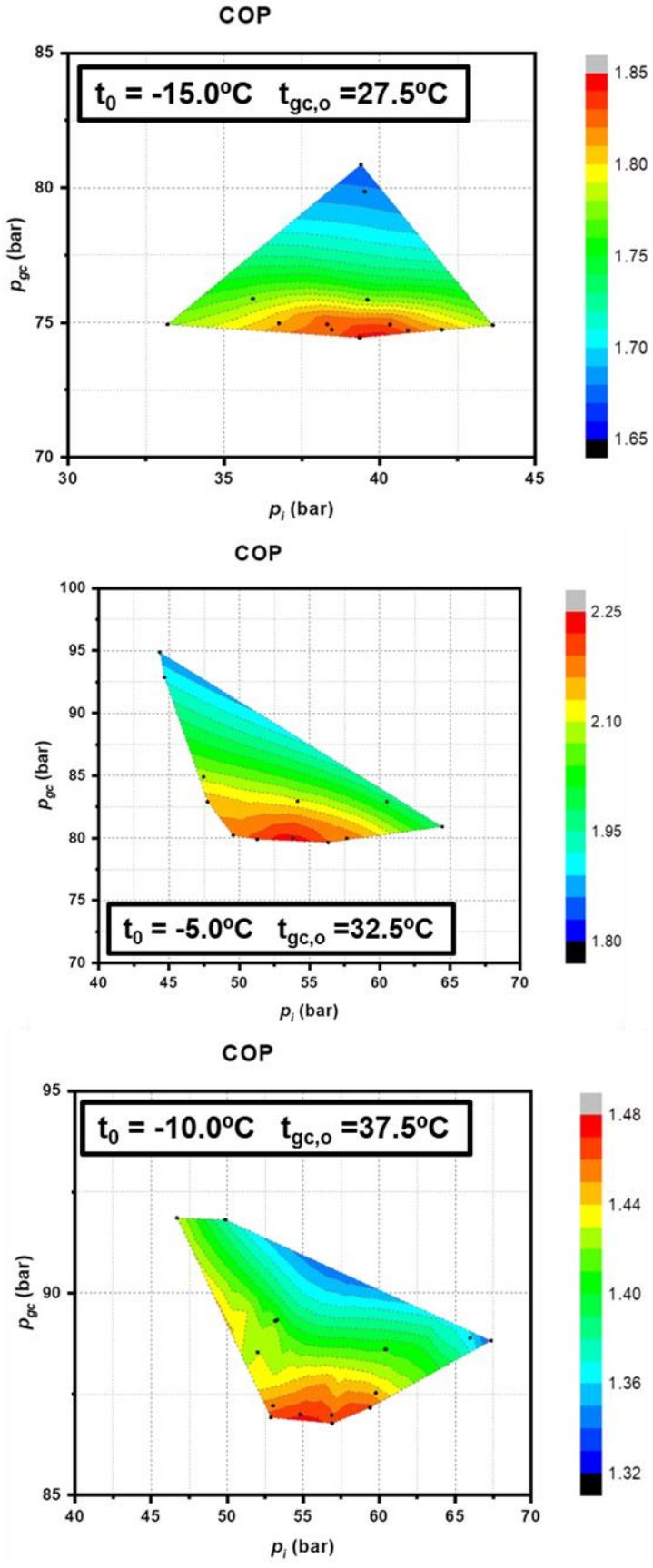


Figure 6. COP evolution for for $t_0$ =-15.0ºC and $t_{gc,o}$=27.5ºC; $t_0$ =-5.0ºC and $t_{gc,o}$=32.5ºC and $t_0$ =-10.0ºC and $t_{gc,o}$=37.5ºC.

To verify the energy balance in the liquid tank and the mass balance, ensuring steady-state conditions, there is only on intermediate pressure that reaches the equilibrium for these conditions. The lower pressure limit may be caused due to the fact that the BP valve is completely open and it is not capable of transferring as much flow as it arrives from the gas-cooler and therefore it is not possible to lower the pressure in the discharge line any further.

The mass balance in the vessel is stated in Eq. ( 5 ). As it can be seen in Figure 1, the mass flow entering the vessel ($\dot{m}_4$) is the sum of the mass flow through the evaporator ($\dot{m}_5$) and the mass flow suctioned by the parallel compressor ($\dot{m}_7$).

$$\dot{m}_4 = \dot{m}_5 + \dot{m}_7 \quad (5)$$

As previously mentioned, in steady-state conditions, the flow extracted through the lower part of the tank is saturated liquid and the flow extracted through the upper part is saturated vapour, so the mass flows can be defined as:

$$\dot{m}_5 = \dot{m}_4 \cdot (1 - x_4) \quad (6)$$

$$\dot{m}_7 = \dot{m}_4 \cdot x_4 \quad (7)$$

Thus, the ratio between the mass flow through the PC and the total mass flow can be determined as:

$$\frac{\dot{m}_7}{\dot{m}_4} = \frac{\dot{m}_4 \cdot x_4}{\dot{m}_4} = x_4 \quad (8)$$

As demonstrated in Eq. ( 8 ) the proportion of mass flow going into the parallel compressor is the vapour quality at the vessel, so it is completely dependent on the intermediate pressure.

Figure 7 shows the ratio between the mass flows (Eq. ( 8 )) as a function of the evaporating level and gas-cooler outlet temperature. It can be observed that when higher the $t_0$ is lower the PC mass flow ratio is. As it will be seen in the following section, when evaporation temperature decreases, the intermediate pressure is lower and the difference between intermediate pressure and gas-cooler pressure increases which lead to a higher $x_4$.

Also, for higher $t_{gc,o}$, the PC mass flow ratio is also higher because for high gas-cooler temperatures, optimum gas-cooler increases while the optimum intermediate pressure decreases when the evaporation temperature decreases. These trends corroborate the theoretical optimization presented by Sarkar and Agrawal [16].

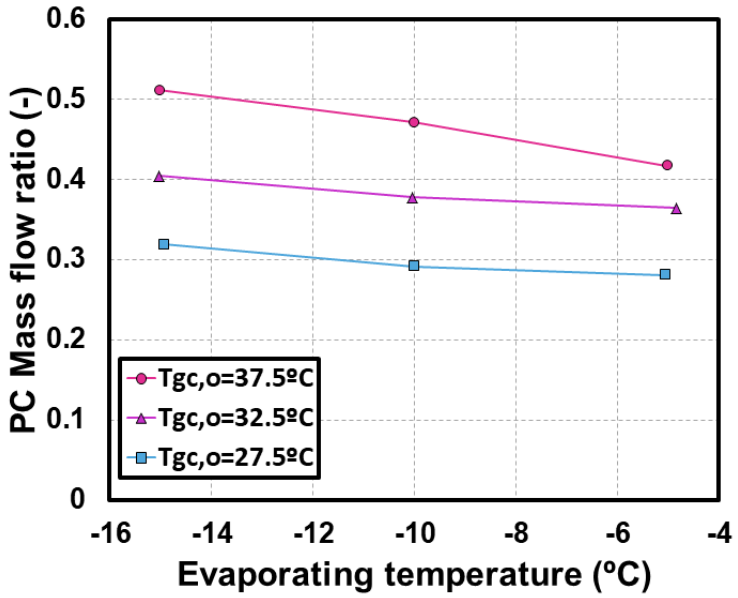


Figure 7. PC Mass flow ratio

## 5. Experimental results at optimum conditions

In this section, the main results are presented for the evaluated conditions: the optimum COP, the cooling capacity and the optimum pressures. The presented results correspond to the experimental points where the highest COP is obtained, which are the optimum conditions. The most important parameters of these tests are summed up in Table 3 as well as the uncertainty of the COP and cooling capacity, which has been calculated using Moffat's method [30]. The measurement devices' accuracies are presented in Table 1. The average measured uncertainty is ±1.24% in $\dot{Q}_0$ and ±1.31% in COP with maximum uncertainty of ±1.40% and ±1.46% respectively. Main operation parameters of the compressors are also included in Table 3 as the volumetric efficiency and the frequency of the IMS compressor. As it can be seen, all the main compressor's overall efficiencies are between 52% and 60% while the overall efficiencies of the parallel compressor are between 48% and 56%, always running below the nominal frequency of 50Hz.

Table 3. Main experimental results and uncertainty measurements.

| | $t_0$ (ºC) | $t_{gc,o}$ (ºC) | $t_{w,in}$ (ºC) | $p_{gc,o}$ (bar) | $p_i$ (bar) | $\dot{m}_0$ (kg·s$^{-1}$) | $P_{CCO2}$ (kW) | $P_{CPC}$ (kW) | $\dot{Q}_0$ (kW) | $\varepsilon(\dot{Q}_0)$ (%) | COP (-) | $\varepsilon$(COP) (%) | $\eta_{main}$ (-) | $\eta_{PC}$ (-) | $f_{PC}$ (Hz) |
|---|---|---|---|---|---|---|---|---|---|---|---|---|---|---|---|
| **E1** | -5.0 | 37.5 | 35.6 | 92.9 | 55.9 | 0.05 | 4.20 | 1.04 | 8.94 | 1.40 | 1.71 | 1.46 | 0.56 | 0.56 | 38 |
| **E2** | -10.0 | 37.6 | 35.6 | 88.8 | 51.4 | 0.04 | 3.90 | 1.23 | 7.71 | 1.27 | 1.50 | 1.33 | 0.55 | 0.55 | 45 |
| **E3** | -15.0 | 37.6 | 36.3 | 88.3 | 49.5 | 0.03 | 3.69 | 1.27 | 6.22 | 1.23 | 1.25 | 1.29 | 0.52 | 0.53 | 45 |
| **E4** | -4.8 | 32.5 | 28.0 | 80.0 | 53.8 | 0.05 | 3.74 | 0.78 | 10.13 | 1.34 | 2.24 | 1.41 | 0.59 | 0.52 | 35 |
| **E5** | -10.0 | 32.4 | 29.7 | 80.9 | 49.6 | 0.04 | 3.66 | 0.85 | 8.28 | 1.25 | 1.84 | 1.32 | 0.56 | 0.51 | 34 |
| **E6** | -15.0 | 32.5 | 30.2 | 80.3 | 46.3 | 0.03 | 3.50 | 0.89 | 6.94 | 1.19 | 1.58 | 1.26 | 0.54 | 0.52 | 35 |
| **E7** | -5.0 | 27.6 | 23.7 | 75.4 | 46.0 | 0.05 | 3.56 | 0.76 | 11.34 | 1.20 | 2.63 | 1.28 | 0.60 | 0.52 | 32 |
| **E8** | -10.0 | 27.6 | 24.3 | 75.0 | 43.3 | 0.04 | 3.51 | 0.77 | 9.47 | 1.16 | 2.22 | 1.24 | 0.57 | 0.48 | 31 |
| **E9** | -14.9 | 27.6 | 24.8 | 74.4 | 39.4 | 0.03 | 3.38 | 0.83 | 7.76 | 1.13 | 1.84 | 1.20 | 0.54 | 0.49 | 33 |

### 5.1. Maximum COP and cooling capacity

Optimum COP is presented in Figure 8 for the three evaporating temperatures as a function of the gas-cooler outlet temperature. As it can be seen, COP is higher when higher the evaporation level is, and it is lower when higher the gas-cooler outlet temperature is. The measured COP is 2.63 at $t_{gc,o}$=27.5ºC, 2.24 at $t_{gc,o}$=32.5ºC and 1.71 at $t_{gc,o}$=37.5ºC for the evaporating level of $t_0$=-5.0ºC. For the evaporating level of $t_0$=-10.0ºC, the measured COP is 2.22 at $t_{gc,o}$=27.5ºC, 1.84 at $t_{gc,o}$=32.5ºC and 1.50 at $t_{gc,o}$=37.5ºC and for the evaporating level of $t_0$=-15.0ºC 1.84, 1.58 and 1.25 respectively.

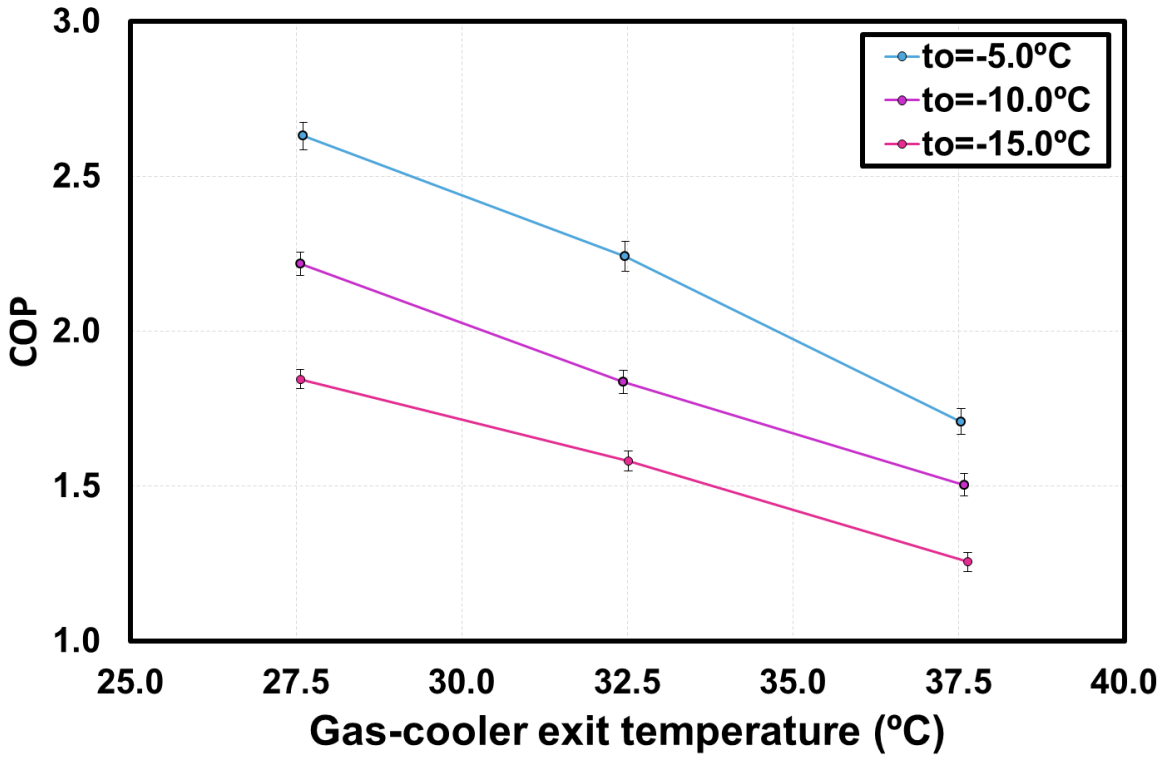


Figure 8. Optimum COP evolution.

Figure 9 shows the cooling capacity of the points with maximum COP. The cooling capacity follows the same trend as the COP, being higher when higher the evaporation level is and when lower the gas-cooler outlet temperature is. The cooling capacity is 11.34 kW at $t_{gc,o}$ =27.5ºC, 10.13 kW at $t_{gc,o}$ =32.5ºC and 8.94 kW at $t_{gc,o}$=37.5ºC for the evaporating level of $t_0$=-5.0ºC. For the evaporating level of $t_0$=-10.0ºC, the measured cooling capacity is 9.47 kW at $t_{gc,o}$ =27.5ºC, 8.28 kW at $t_{gc,o}$=32.5ºC and 7.71 kW at $t_{gc,o}$ =37.5ºC and for the evaporating level of $t_0$=-15.0ºC 7.76 kW, 6.94 kW and 6.22 kW respectively.

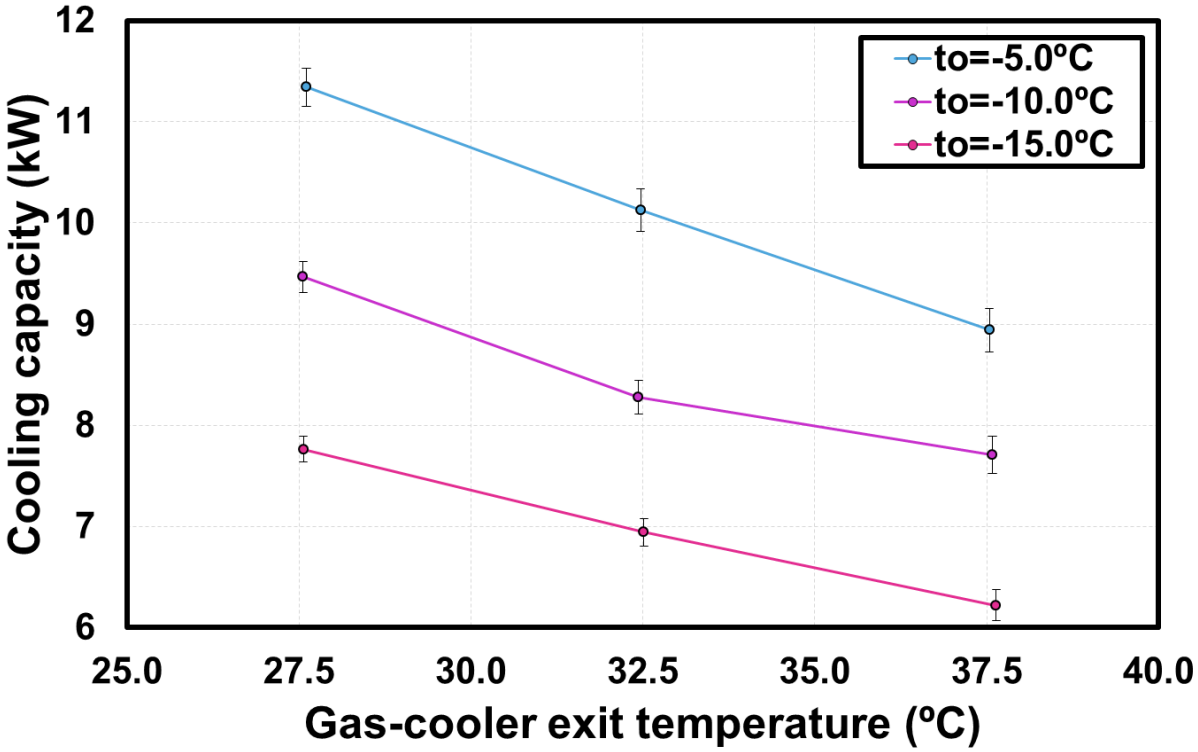


Figure 9. Evolution of the cooling capacity.

### 5.2. Optimum pressures

The COP of the plant depends on the gas-cooler pressure but also on the intermediate pressure that is the pressure of the liquid tank. Gas-cooler pressure can be regulated thanks to the back-pressure valve and the pressure in the vessel should be regulated by the parallel compressor's speed.

Figure 10 shows the optimum gas-cooler pressure and the optimum intermediate pressures. As it can be seen, gas-cooler pressure strongly depends on the gas-cooler outlet temperature, being higher when higher the temperature is but it practically does not depend on the evaporation level.

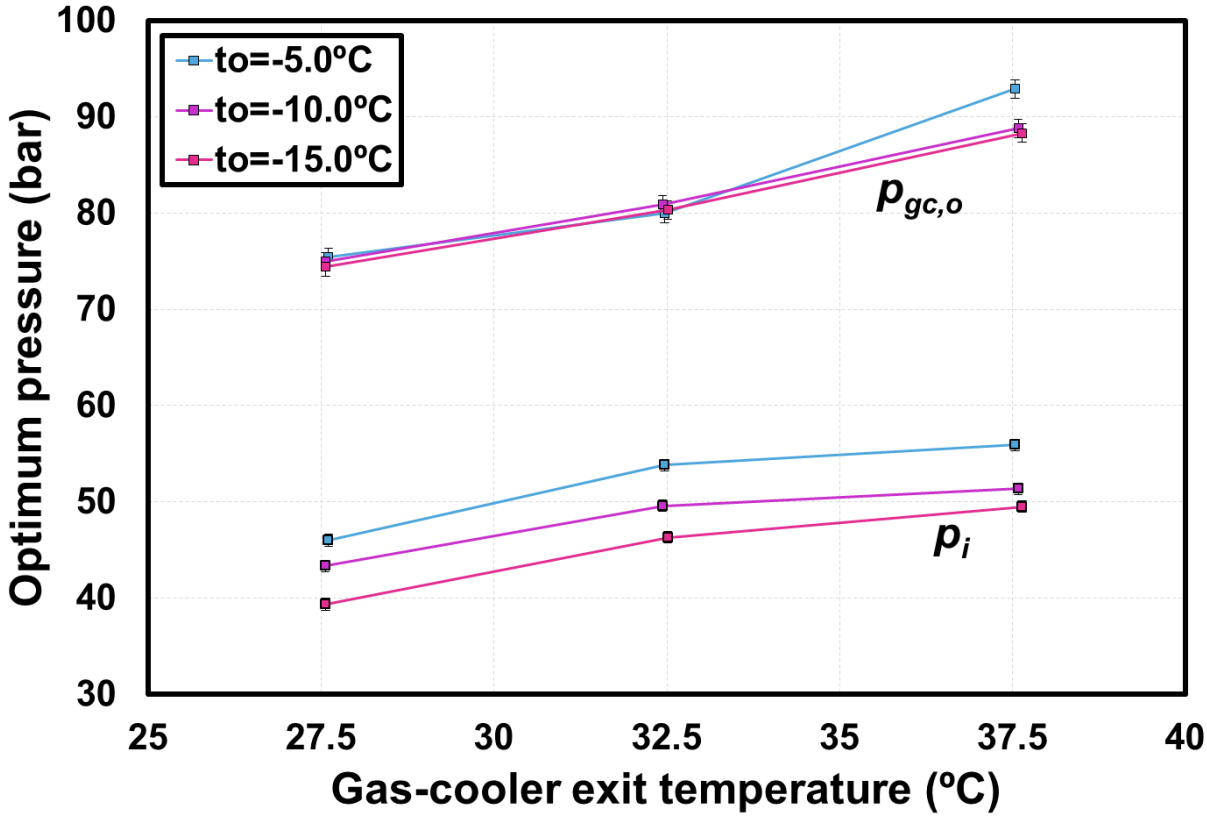


Figure 10. Optimum gas-cooler and intermediate pressures.

The obtained gas-cooler pressures have the same trend as the pressures obtained by Sarkar and Agrawal [16]. It is dependent on the gas-cooler temperature and it is higher when higher the temperature is. Also, as presented by Sarkar and Agrawal, it is practically independent on the evaporation level. When regarding the highest evaporation level (E1 in Table 3), a slight influence of the evaporation temperature on the discharge pressure can be observed. This coincides with the operating limits of the system, presented by Chesi et al. [25], where the gas-cooler pressure increases for high ambient temperatures for the highest evaporation levels.

The intermediate pressure has a different trend. it depends both on the gas-cooler outlet temperature and the evaporating temperature as it can be seen in Figure 10. The pressure is higher when higher the evaporation temperature and the gas-cooler outlet temperature are. The obtained trends on the intermediate pressure are also observed in the theoretical study of the $CO_2$ cycle with parallel compression performed by Sarkar and Agrawal [16].

In the following section the correlations to obtain both pressures are presented. They are also compared to the correlations proposed by Sarkar and Agrawal [16] in their theoretical study.

### 5.5. Correlations

The following correlations are obtained from the experimental data and they allow calculating the optimal working pressures to obtain maximum COP depending on the evaporation and gas-cooler outlet temperature conditions. Correlations have been obtained using an adjustment of least-squares.

### 5.5.1. Optimum gas-cooler pressure

Gas-cooler pressure's correlation is defined in Eq. ( 9 ) and it is a function of the gas-cooler outlet temperature and the evaporation temperature.

$$p_{gc} = 101.3 - 3.064 \cdot t_{gc} - 1.1 \cdot t_0 + 0.0762 \cdot t_{gc}^2 + 0.0392 \cdot t_{gc} \cdot t_0 \quad (9)$$

The range of application of this correlation is for temperatures of gas-cooler exit between 27.5 °C and 37.5 °C and evaporation temperatures between −15.0 °C and −5.0 °C. The root-mean-square deviation of the correlation is 1.213 bar.

Figure 11 shows the comparison of the optimum gas-cooler pressure obtained by the correlation proposed in Eq. ( 9 ) with the correlation proposed by Sarkar and Agrawal [16] for different evaporation temperatures and a range of gas-cooler exit temperatures between 30 and 37ºC, where both correlations can be applied. As it can be observed, both pressures are quite similar but those corresponding to the lower temperatures have a slightly higher discrepancy (up to 4 bar for $t_{gc,o}$ = 30ºC). Even so, we can affirm that the trend obtained by Sarkar and Agrawal [16] is experimentally corroborated with the results presented in this work.

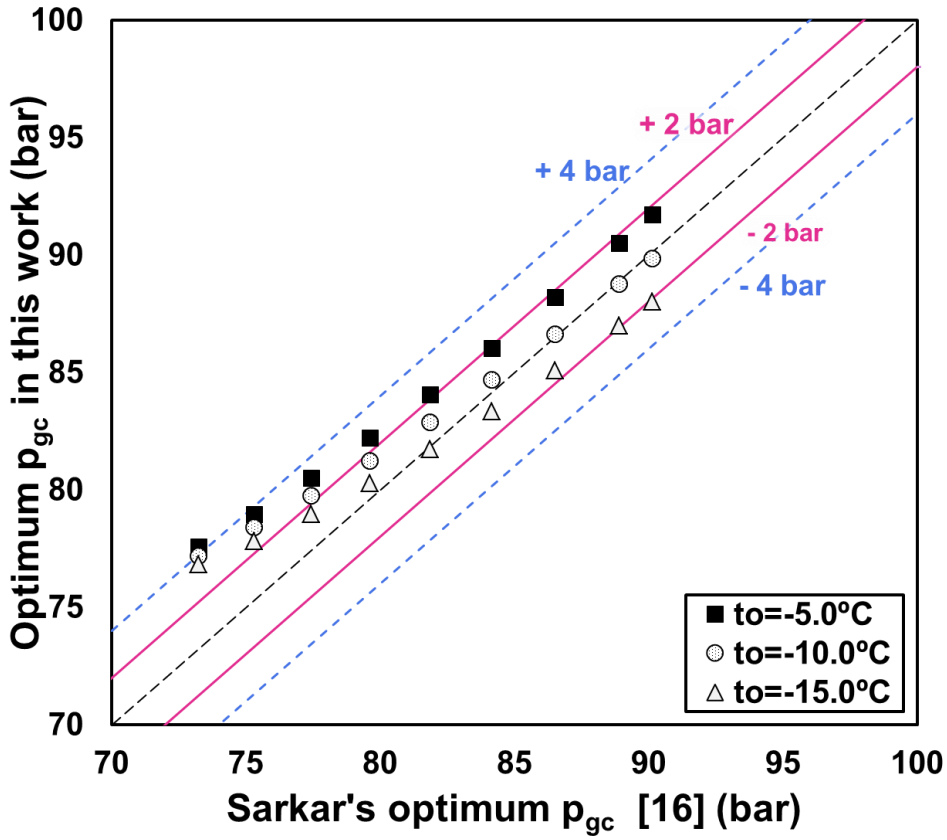


Figure 11. Comparison of the optimum gas-cooler pressure obtained by Sarkar's correlation [16] with the optimum pressures obtained experimentally.

### 5.5.2. Optimum intermediate pressure

The optimum intermediate pressure can be calculated with Eq. ( 10 ). The range of application of this correlation is for evaporation temperatures between −15.0 °C and −5.0 °C and temperatures of gas-cooler exit between 27.5 °C and 37.5 °C. The root-mean-square deviation of the correlation is 0.6761 bar.

$$p_i = -74.87 + 7.175 \cdot t_{gc} + 0.7716 \cdot t_0 - 0.0962 \cdot t_{gc}^2 - 0.0027 \cdot t_0 \cdot t_{gc} \quad (10)$$

## 6. Conclusions

The experimental optimization of a $CO_2$ transcritical refrigeration plant with parallel compression is presented in this work. The evaluation covered three evaporating levels (-5.0ºC, -10.0ºC and -15.0ºC) and the gas-cooler exit temperatures of 27.5ºC, 32.5ºC and 37.5ºC at steady-state conditions. The main compressor worked at nominal speed while the parallel compressor's speed has been modified in order to obtain the optimum intermediate pressure.

The results obtained in this work corroborate the trends presented in the theoretical optimization of Sarkar and Agrawal [16]. Also, the tank pressure limit has been demonstrated experimentally.

The experimental tests have allowed to demonstrate the existence of a maximum COP, obtained for the optimum conditions of gas-cooler and intermediate pressures, that varies depending on the test conditions. The optimum COP goes from 1.71 to 2.63 for the evaporating temperature of -5.0ºC, from 1.50 to 2.22 for the evaporating temperature of -10.0ºC and from 1.25 to 1.84 for -15.0ºC. The cooling capacity from 8.94 kW to 11.34 kW for the evaporating temperature of -5.0ºC, from 7.71 kW to 9.47 kW for -10.0ºC and from 6.22 kW to 7.76 kW for -15.0ºC. The optimum pressure is strongly dependent on the gas-cooler outlet temperature, being higher when higher the temperature is, whereas it practically does not depend on the level of evaporation for the evaluated evaporation temperatures. On the other hand, the optimum intermediate pressure depends on both, the gas-cooler outlet temperature and the evaporation temperature, being higher when higher the evaporation level and the gas-cooler outlet temperature are.

Two general expressions have been stated from the experimental data to determine the optimum gas-cooler and intermediate pressures for $CO_2$ single-stage transcritical refrigeration plants with parallel compression, only depending on the evaporation level and the gas-cooler outlet temperature. The correlation obtained to determine the gas-cooler pressure is compared to the correlation proposed by Sarkar and Agrawal [16] corroborating experimentally the trends presented in Sarkar and Agrawal's theoretical study.

Furthermore, further research is needed to study the physical limitations that have been found in the experimental operation of this plant.

## Acknowledgements

The authors thank the Ministerio de Educación, Cultura y Deporte (Spain) grant FPU16/00151; the Ministerio de Ciencia y Tecnología (Spain) project RTI2018-093501-B-C21, and the Jaume I University (Spain), project UJI-B2019-56 for financing this research work.

## References

[1] UNEP/TEAP, The implications to the Montreal Protocol of the inclusion of HFCs and PFCs in the Kyoto Protocol, in, United States, 1999.
[2] European Commission, Regulation (EU) No 517/2014 of the European Parliament and of the Council of 16 April 2014 on fluorinated greenhouse gases and repealing Regulation (EC) No 842/2006., (2014).
[3] Hafner A., Hemmingsen A. K. T., Ven A. van de, R744 refrigeration system configurations for supermarkets in warm climates, in: 3rd IIR International Conference on Sustainability and the Cold Chain. Proceedings, International Institute of Refrigeration, London, UK, 2014.
[4] N. Lawrence, S. Elbel, Experimental investigation on control methods and strategies for off-design operation of the transcritical R744 two-phase ejector cycle, International Journal of Refrigeration, (2019).

[5] N. Lawrence, S. Elbel, Experimental study on control methods for transcritical CO2 two-phase ejector systems at off-design conditions, in: Refrigeration Science and Technology, 2016, pp. 511-518.
[6] R. Llopis, L. Nebot-Andrés, D. Sánchez, J. Catalán-Gil, R. Cabello, Subcooling methods for CO2 refrigeration cycles: A review, International Journal of Refrigeration, 93 (2018) 85-107.
[7] J. Rigola, N. Ablanque, C.D. Pérez-Segarra, A. Oliva, Numerical simulation and experimental validation of internal heat exchanger influence on CO2 trans-critical cycle performance, International Journal of Refrigeration, 33 (2010) 664-674.
[8] R. Llopis, L. Nebot-Andrés, R. Cabello, D. Sánchez, J. Catalán-Gil, Experimental evaluation of a CO2 transcritical refrigeration plant with dedicated mechanical subcooling, International Journal of Refrigeration, 69 (2016) 361-368.
[9] L. Nebot-Andrés, D. Sánchez, D. Calleja-Anta, R. Cabello, R. Llopis, Experimental determination of the optimum working conditions of a commercial transcritical CO2 refrigeration plant with a R-152a dedicated mechanical subcooling, International Journal of Refrigeration, (2020).
[10] J. Bush, M. Beshr, V. Aute, R. Radermacher, Experimental evaluation of transcritical CO2 refrigeration with mechanical subcooling, Science and Technology for the Built Environment, 23 (2017) 1013-1025.
[11] M. Beshr, J. Bush, V. Aute, R. Radermacher, Steady state testing and modeling of a CO2 two-stage refrigeration system with mechanical subcooler, in: Refrigeration Science and Technology, 2016, pp. 893-900.
[12] L. Nebot-Andrés, J. Catalán-Gil, D. Sánchez, D. Calleja-Anta, R. Cabello, R. Llopis, Experimental determination of the optimum working conditions of a transcritical CO2 refrigeration plant with integrated mechanical subcooling, International Journal of Refrigeration, 113 (2020) 266-275.
[13] M. Karampour, S. Sawalha, Integration of heating and air conditioning into a CO2 trans-critical booster system with parallel compression Part I: Evaluation of key operating parameters using field measurements, in: Refrigeration Science and Technology, 2016, pp. 323-331.
[14] C. Aprea, A. Greco, A. Maiorino, The application of a desiccant wheel to increase the energetic performances of a transcritical cycle, Energy Conversion and Management, 89 (2015) 222-230.
[15] A. Arora, N.K. Singh, S. Monga, O. Kumar, Energy and exergy analysis of a combined transcritical CO2 compression refrigeration and single effect H2O-LiBr vapour absorption system, International Journal of Exergy, 9 (2011) 453-471.
[16] J. Sarkar, N. Agrawal, Performance optimization of transcritical CO2 cycle with parallel compression economization, International Journal of Thermal Sciences, 49 (2010) 838-843.
[17] S. Sawalha, M. Karampour, J. Rogstam, Field measurements of supermarket refrigeration systems. Part I: Analysis of CO2 trans-critical refrigeration systems, Applied Thermal Engineering, 87 (2015) 633-647.
[18] M. Karampour, S. Sawalha, Integration of heating and air conditioning into a CO2 trans-critical booster system with parallel compression part II: Performance analysis based on field measurements, in: Refrigeration Science and Technology, 2016, pp. 332-340.
[19] P. Gullo, B. Elmegaard, G. Cortella, Energy and environmental performance assessment of R744 booster supermarket refrigeration systems operating in warm climates, International Journal of Refrigeration, 64 (2016) 61-79.
[20] K.M. Tsamos, Y.T. Ge, I. Santosa, S.A. Tassou, G. Bianchi, Z. Mylona, Energy analysis of alternative CO2 refrigeration system configurations for retail food applications in moderate and warm climates, Energy Conversion and Management, 150 (2017) 822-829.
[21] A. Polzot, P. D'Agaro, G. Cortella, Energy Analysis of a Transcritical CO2 Supermarket Refrigeration System with Heat Recovery, Energy Procedia, 111 (2017) 648-657.
[22] P. Gullo, K. Tsamos, A. Hafner, Y. Ge, S.A. Tassou, State-of-the-art technologies for transcritical R744 refrigeration systems – a theoretical assessment of energy advantages for European food retail industry, Energy Procedia, 123 (2017) 46-53.
[23] J. Catalán-Gil, D. Sánchez, R. Llopis, L. Nebot-Andrés, R. Cabello, Energy evaluation of multiple stage commercial refrigeration architectures adapted to F-gas regulation, Energies, 11 (2018).
[24] S. Minetto, L. Cecchinato, M. Corradi, E. Fornasieri, C. Zilio, A. Schiavon, Theoretical and experimental analysis of a CO2 refrigerating cycle with two-stage throttling and suction of the flash vapour by an auxiliary compressor, in: IIR International conference on thermophysical properties and transfer processes of refrigerants, Vicenza (Italy), 2005.

[25] A. Chesi, F. Esposito, G. Ferrara, L. Ferrari, Experimental analysis of R744 parallel compression cycle, Applied Energy, 135 (2014) 274-285.
[26] B. Bella, N. Kaemmer, Experimental Performance of Carbon Dioxide Compressor with Parallel Compression, in: DKV-Tagung, Aachen (Germany), 2011.
[27] E.W. Lemmon, M.L. Huber, M.O. McLinden, REFPROP, NIST Standard Reference Database 23, v.9.1. National Institute of Standards, Gaithersburg, MD, U.S.A., (2013).
[28] L. Cecchinato, M. Chiarello, M. Corradi, E. Fornasieri, S. Minetto, P. Stringari, C. Zilio, Thermodynamic analysis of different two-stage transcritical carbon dioxide cycles, International Journal of Refrigeration, 32 (2009) 1058-1067.
[29] M.M. Hazarika, Studies on a CO2 based summer air conditioning system with single and multiple expansion valves, in: Department of mechanical engineering Vol. Doctor of Philosophy, Indian Institute of Technology Kharagpur, 2020, pp. 158.
[30] R.J. Moffat, Using Uncertainty Analysis in the Planning of an Experiment, Journal of Fluids Engineering, 107 (1985) 173-178.